Genome-wide RNAi screen of Ca^{2+} influx identifies genes that regulate Ca^{2+} release-activated Ca^{2+} channel activity

Shenyuan L. Zhang*, Andriy V. Yeromin*, Xiang H.-F. Zhang†, Ying Yu*, Olga Safrina*, Aubin Penna*, Jack Roos‡, Kenneth A. Stauderman‡, and Michael D. Cahalan*§

*Department of Physiology and Biophysics and Center for Immunology, University of California, Irvine, CA 92697; †Department of Biological Sciences, Columbia University, New York, NY 10027; and ‡TorreyPines Therapeutics, Inc., La Jolla, CA 92037

Communicated by Bertil Hille, University of Washington, Seattle, WA, April 19, 2006 (received for review April 11, 2006)

Recent studies by our group and others demonstrated a required and conserved role of *Stim* in store-operated Ca^{2+} influx and Ca^{2+} release-activated Ca^{2+} (CRAC) channel activity. By using an unbiased genome-wide RNA interference screen in *Drosophila* S2 cells, we now identify 75 hits that strongly inhibited Ca^{2+} influx upon store emptying by thapsigargin. Among these hits are 11 predicted transmembrane proteins, including *Stim*, and one, *olf186-F*, that upon RNA interference-mediated knockdown exhibited a profound reduction of thapsigargin-evoked Ca^{2+} entry and CRAC current, and upon overexpression a 3-fold augmentation of CRAC current. CRAC currents were further increased to 8-fold higher than control and developed more rapidly when *olf186-F* was cotransfected with *Stim*. *olf186-F* is a member of a highly conserved family of four-transmembrane spanning proteins with homologs from *Caenorhabditis elegans* to human. The endoplasmic reticulum (ER) Ca^{2+} pump sarco-/ER calcium ATPase (SERCA) and the single transmembrane-soluble *N*-ethylmaleimide-sensitive (NSF) attachment receptor (SNARE) protein Syntaxin5 also were required for CRAC channel activity, consistent with a signaling pathway in which *Stim* senses Ca^{2+} depletion within the ER, translocates to the plasma membrane, and interacts with *olf186-F* to trigger CRAC channel activity.

capacitative calcium entry (CCE) | genome-wide screen | CRAC channel | RNA interference | store-operated calcium (SOC) influx

Patch–clamp experiments have identified the biophysical characteristics of Ca^{2+} release-activated Ca^{2+} (CRAC) channels in lymphocytes and other human cell types (1, 2). Despite the acknowledged functional importance of store-operated Ca^{2+} (SOC) influx in cell biology (2) and of CRAC channels for immune cell activation (3), the intrinsic channel components and signaling pathways that lead to channel activation remain unidentified. In previous work (4), we demonstrated that SOC influx in S2 cells occurs through a channel that shares biophysical properties with CRAC channels in human T lymphocytes. In a medium-throughput RNA interference (RNAi) screen targeting 170 candidate genes in S2 cells, we discovered an essential conserved role of *Stim* and the mammalian homolog STIM1 in SOC influx and CRAC channel activity (5). STIM1 and STIM2 also were identified in an independently performed screen of HeLa cells by using the *Drosophila* enzyme Dicer to generate small interfering RNA species from dsRNA (6). *Drosophila Stim* and the mammalian homolog STIM1 appear to play dual roles in the CRAC channel activation sequence, sensing the luminal Ca^{2+} store content through an EF hand motif and trafficking from an endoplasmic reticulum (ER)-like localization to the plasma membrane to trigger CRAC channel activity (6–8). However, as single-pass transmembrane proteins, *Stim* and its mammalian homolog STIM1 are unlikely to form the CRAC channel itself. To search systematically for additional components of the CRAC channel, and to analyze the signaling network and other required factors that lead to SOC channel activity, we devised and performed a genome-wide screen on S2 cells based on a fluorescence assay of Ca^{2+} influx. The library at Harvard's *Drosophila* RNAi Screening Center (DRSC) of 23,845 dsRNA amplicons has been used in several functional screens (9–14).

A very recent report identified a genetic defect in patients with severe combined immune deficiency (SCID) (15). The screen in this study made use of the ability of thapsigargin (TG) to send GFP-tagged nuclear factor of activated T cells (NFAT) to the nucleus in S2 cells, providing an assay for disruption of signaling anywhere in the cascade from elevated $[Ca^{2+}]_i$ to calcineurin activation and nuclear relocalization of NFAT. The fly gene *olf186-F* (named *Orai*) was identified in the screen, and a human homolog on chromosome 12 was shown to be mutated in SCID patients, resulting in the loss of CRAC channel activity. Heterologous expression of the wild-type human homolog, which was named Orai1, restored CRAC channel activity in SCID T cell lines.

Here, based on direct Ca^{2+} influx measurements in a genome-wide screen, we identify several genes that are required for CRAC channel function in S2 cells. Our results confirm the functional requirement of *olf186-F* (*Orai*) for Ca^{2+} signaling and extend these results to investigate effects of knockdown and overexpression on CRAC channel activity. We also show that the sarco-/ER calcium ATPase (SERCA) pump and the trafficking protein Syntaxin 5 are required for CRAC channel activity.

Results

Genome-Wide Screen for SOC Influx. Each well of 63 separate 384-well plates contained an individual dsRNA amplicon. Ca^{2+}-indicator fluorescence measurements were made in each well to monitor cytosolic Ca^{2+} ($[Ca^{2+}]_i$) before (basal) and after [capacitive calcium entry (CCE)] addition of TG. TG inhibits SERCA pump-mediated reuptake of Ca^{2+} into cellular stores, depleting them and triggering CCE in S2 cells (4, 16), as well as in mammalian cells (2). Hits in the screen were defined by significantly reduced CCE/basal values, as described in *Methods* and illustrated by a tail in the histogram shown in Fig. 1*A*. The "top 10 hits," with strong suppressive effects comparable with the average value of the *Stim* positive control (CCE/basal ≈ 1.3), were selected for further evaluation (Fig. 1*B*; see also Table 1, which is published as supporting information on the PNAS web site). Among the 75 filtered hits with z-scores of CCE/basal < -3 (see Table 2, which is published as supporting information on the PNAS web site), only 11 contained transmembrane seg-

Conflict of interest statement: No conflicts declared.

Abbreviations: CCE, capacitive calcium entry; CRAC, Ca^{2+} release-activated Ca^{2+}; ER, endoplasmic reticulum; RNAi, RNA interference; SERCA, sarco-/ER calcium ATPase; SNARE, single transmembrane-soluble *N*-ethylmaleimide-sensitive attachment receptor; SOC, store-operated Ca^{2+}; TG, thapsigargin.

§To whom correspondence should be addressed. E-mail: mcahalan@uci.edu.

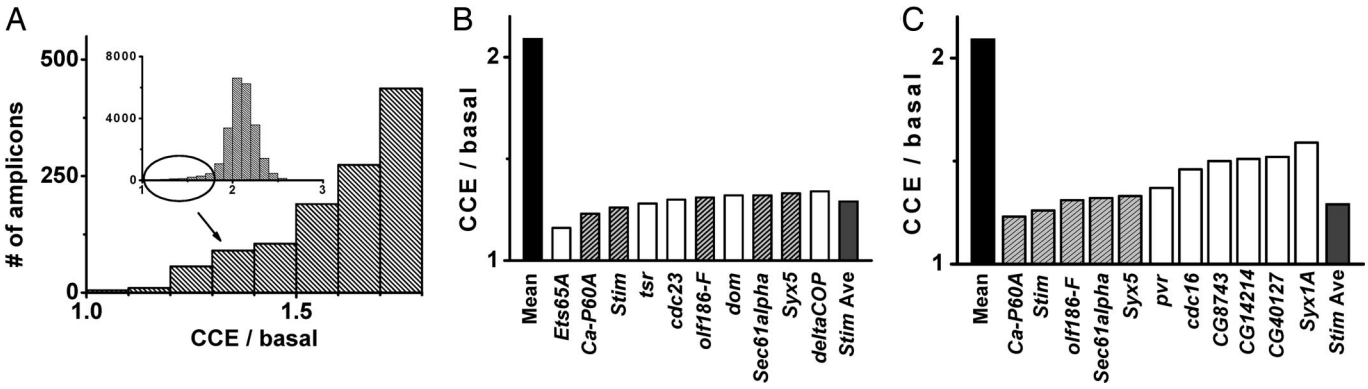

Fig. 1. Identification of genes involved in store-operated calcium entry. (*A*) The effect of individual gene silencing on TG-evoked Ca^{2+} entry (CCE) relative to basal Ca^{2+}, displayed as a histogram. (*Inset*) The distribution of averaged CCE/basal values for each well. Low values of CCE/basal are enlarged to show the tail of the distribution, representing amplicons that dramatically suppressed TG-evoked calcium entry. (*B*) The top 10 hits with strongest effect on TG-evoked Ca^{2+} influx. Averaged values of CCE/basal are shown for all 48,384 wells tested in the assay (''mean''), for the top 10 hits from the screen, and for the positive control well that contained *Stim* dsRNA in each assay plate (''*Stim* Ave''). Striped bars represent hits with transmembrane regions. (*C*) Transmembrane (TM) protein hits.

ments, as shown in Fig. 1*C*. Among these hits, the five strongest are annotated in Flybase (www.flybase.org) as *Ca-P60A*, *Stim*, *olf186-F*, *sec61alpha*, and *Syx5*.

The consistent suppressive effect of *Stim* dsRNA validates the present screen. However, *Stim* is unlikely to constitute the CRAC channel, because multiple transmembrane segments are found in all known ion-channel pore-forming subunits. The protein product of *sec61alpha* is a subunit of the translocon complex, which recognizes and delivers newly synthesized membrane proteins into ER, and may be a hit in this screen by altering synthesis or localization of other essential components. *Ca-P60A* is the SERCA pump gene in fly, whose products are located in the ER for filling/refilling the Ca^{2+} store. *Syx5* generates a single transmembrane-soluble *N*-ethylmaleimide-sensitive (NSF) at-

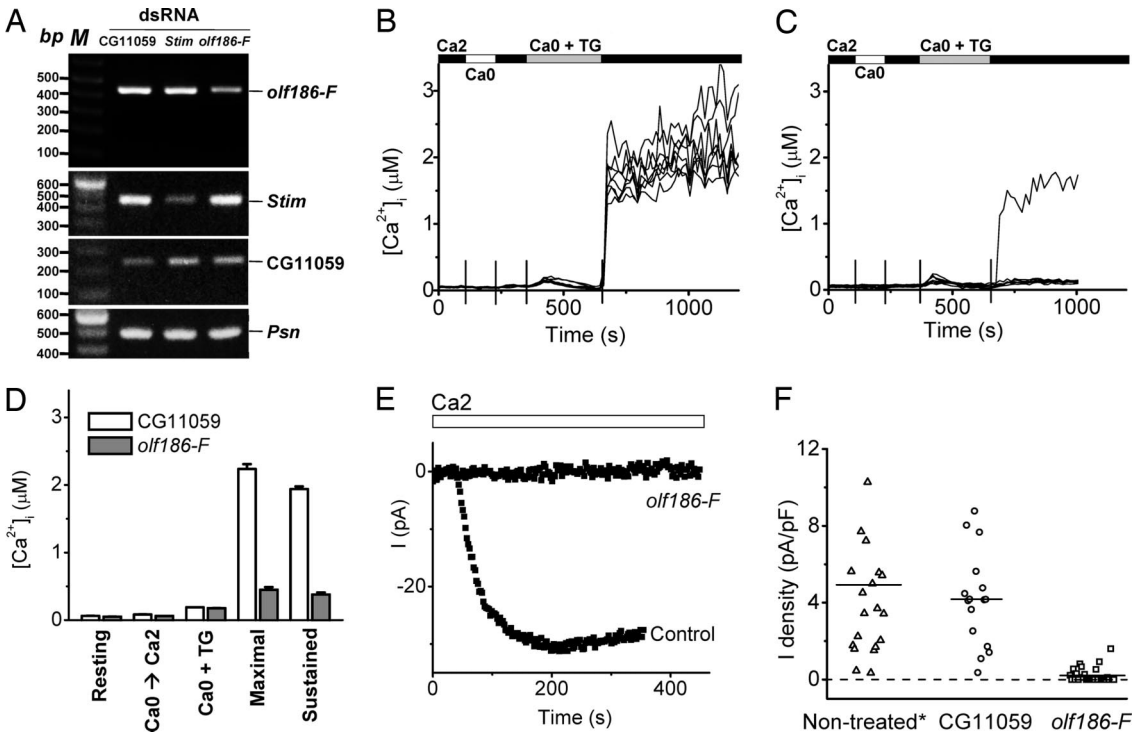

Fig. 2. Suppression of TG-dependent Ca^{2+} influx and CRAC current by *olf186-F* dsRNA. (*A*) Reduction of *olf186-F* mRNA expression in *olf186-F* dsRNA-treated cells. RT-PCR analysis on *olf186-F*, *Stim*, CG11059, and a control gene, *Presenilin* (*Psn*). (*B*) $[Ca^{2+}]_i$ in eight representative S2 cells treated with CG11059 dsRNA. Solution exchanges are indicated. (*C*) $[Ca^{2+}]_i$ in eight cells treated with *olf186-F* dsRNA. (*D*) Averaged $[Ca^{2+}]_i$ values ± SEM for control cells ($n = 195$ cells in three experiments; white bars) and *olf186-F* dsRNA-treated cells ($n = 189$ in four experiments; gray bars): resting $[Ca^{2+}]_i$, peak value upon readdition of 2 mM external Ca^{2+} before TG treatment (Ca0 → Ca2), peak $[Ca^{2+}]_i$ during TG-evoked release transient (Ca0 + TG), and maximal and sustained (3 min) $[Ca^{2+}]_i$ after readdition of 2 mM external Ca^{2+}. (*E*) Representative time course of whole-cell currents recorded in control cells treated with CG11059 dsRNA and in cells treated with *olf186-F* dsRNA. (*F*) Suppression of CRAC current by *olf186-F* dsRNA pretreatment. Each point represents the maximal inward CRAC current density (pA/pF) in a single cell, plotted as absolute values in consecutive order from left to right within three groups of cells: untreated, cells treated with dsRNA to suppress CG11059, or *olf186-F* ($P < 5 \times 10^{-6}$ compared with either control group). The untreated cell group includes two cells each with current density >12 pA/pF. Horizontal lines indicate the mean value of current density in each group.

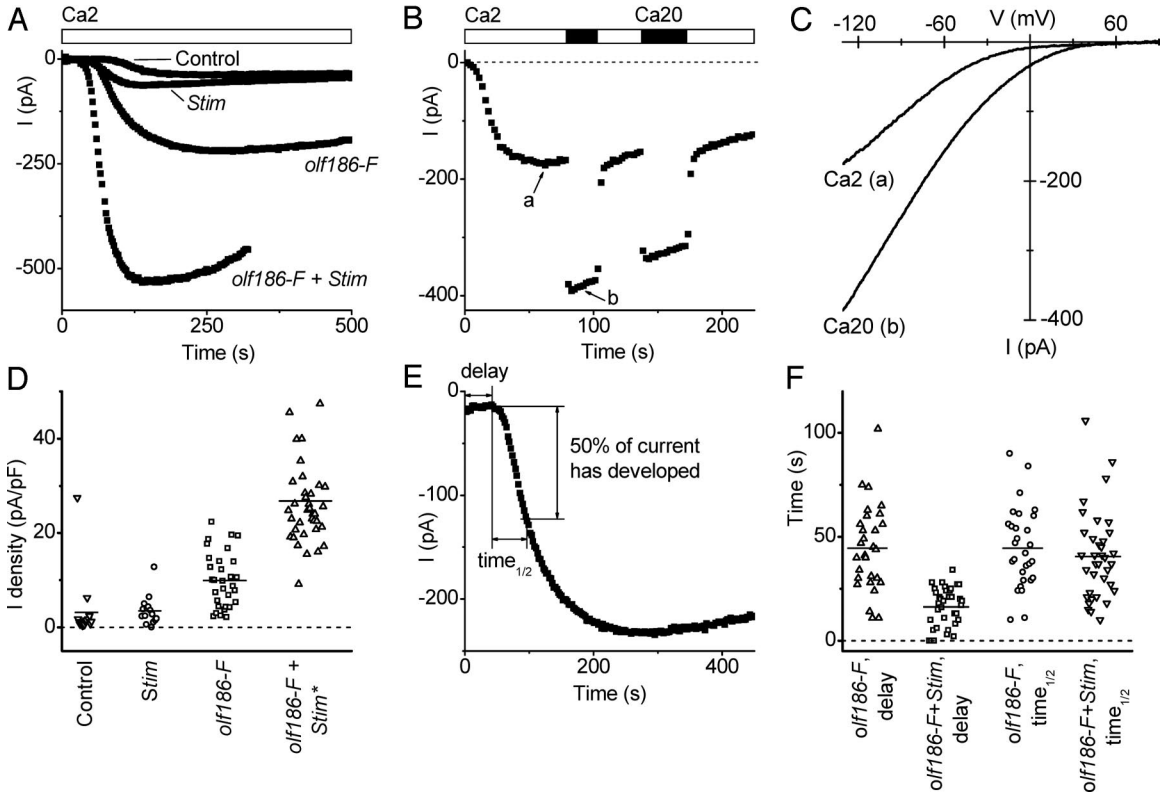

Fig. 3. Overexpression of *olf186-F* leads to increased CRAC currents in S2 cells. (*A*) Representative CRAC currents in S2 cells transfected with GFP only (control), *Stim*, *olf186-F*, and *olf186-F* plus *Stim*. (*B*) Ca^{2+} current in *olf186-F* + *Stim* cotransfected cell. Arrows a and b indicate the time corresponding to current–voltage curves in *C*. (*C*) Current–voltage relationship of CRAC current in the same cell. (*D*) CRAC current density in transfected S2 cells, plotted as in Fig. 2*F*, within four groups of cells: GFP-transfected control; *Stim* and GFP cotransfected (not significantly different from controls); *olf186-F* and GFP cotransfected ($P < 10^{-3}$); and *olf186-F*, *Stim*, and GFP cotransfected ($P < 5 \times 10^{-6}$). The group of cells cotransfected by *olf186-F*, *Stim*, and GFP includes one cell with current density >50 pA/pF. (*E*) Method to analyze kinetics of CRAC current development. (*F*) Effect of cotransfected *Stim* on delay kinetics. Delay times are significantly reduced ($P < 5 \times 10^{-6}$), but $time_{1/2}$ values are not altered when *Stim* is expressed together with *olf186-F*, compared with *olf186-F* alone.

tachment receptor (SNARE) protein (Syntaxin 5), which is essential for vesicle fusion and may modulate CCE by altered protein trafficking rather than serving as the channel pore. Thus, among the top 10 hits, *olf186-F* is the only gene of unknown structure and function that is predicted to contain multiple transmembrane segments.

Effects of *olf186-F* Knockdown and Overexpression on Ca^{2+} Influx and CRAC Currents in Single Cells. To clarify effects of suppressing *olf186-F* at the level of single cells, we examined Ca^{2+} signaling and CRAC currents in cells treated with dsRNA for *olf186-F*, in comparison with untreated cells or with cells treated with dsRNA for CG11059, an irrelevant cell adhesion molecule (5), as controls. RT-PCR showed >50% decrease of *olf186-F* mRNA expression, compared with controls (Fig. 2*A*). Fig. 2*B* illustrates ratiometric fura-2 $[Ca^{2+}]_i$ measurements before and after TG-evoked store depletion in eight individual control cells. Addition of TG in zero-Ca^{2+} solution to deplete the store elicited a Ca^{2+} release transient caused by net leak of Ca^{2+} from the store when the reuptake pump is blocked. Upon readdition of external Ca^{2+}, a robust Ca^{2+} signal was observed in every cell. In cells pretreated with *olf186-F* dsRNA, neither the resting $[Ca^{2+}]_i$ level nor the release transient were significantly altered, but the rise in $[Ca^{2+}]_i$ upon readdition of external Ca^{2+} was strongly suppressed in the vast majority of the individual cells (Fig. 2*C*). Fig. 2*D* clearly demonstrates that suppression of *olf186-F* effectively inhibits both the early and sustained components of Ca^{2+} entry evoked by TG at the single-cell level. Comparable inhibition was obtained in cells pretreated with *Stim* dsRNA as a positive control (data not shown), consistent with our previous report (5).

Patch–clamp experiments confirmed a dramatic suppression of CRAC currents after knockdown of *olf186-F* (Fig. 2 *E* and *F*). CRAC current normally develops after establishing the whole-cell recording configuration as the cytoplasm is dialyzed by a pipette solution containing a strong Ca^{2+} chelator to reduce cytosolic $[Ca^{2+}]_i$ and deplete internal stores. With this method of "passive stores depletion," current increases after an initial delay to a maximum value before declining slowly. However, in the majority of cells pretreated with *olf186-F* dsRNA, CRAC current was completely suppressed, as illustrated by the representative traces in Fig. 2*E* and by a chart of CRAC current densities (Fig. 2*F*). As we showed previously for *Stim* (5), *olf186-F* expression is required for normal CRAC channel activity.

To examine further the function of *olf186-F*, we cloned its full-length cDNA from S2 cells and inserted it into a *Drosophila* expression vector. The *olf186-F* clone was overexpressed with or without a cotransfected *Stim* clone in S2 cells, by using a cotransfected GFP construct for identification of transfected cells. Increased expression levels of *olf186-F* and *Stim* after separate transfections or cotransfection were verified by RT-PCR (see Fig. 6*A*, which is published as supporting information on the PNAS web site). Fig. 3*A* illustrates the time course of current development after break-in to achieve whole-cell recording in four representative cells. Expression of *Stim* by itself had no significant effect on current amplitude compared with control, untransfected cells. However, when *olf186-F* was overexpressed, CRAC current increased significantly, and when

olf186-F was coexpressed with *Stim*, CRAC current was further enhanced. The induced current after cotransfection of *olf186-F* with *Stim* exhibited Ca^{2+} selectivity and current–voltage shapes indistinguishable from native CRAC current (Fig. 3 *B* and *C*). When external Ca^{2+} was elevated 10-fold, the current magnitudes approximately doubled, as is the case for native CRAC current in S2 cells (4), and current–voltage curves had the same inwardly rectifying characteristic. Fig. 3*D* illustrates CRAC current densities for individual cells in each group of transfected cells. Overexpression of *olf186-F* increased the average current density 3-fold, and although *Stim* by itself did not alter current density, cotransfection with *olf186-F* produced a remarkable 8-fold enhancement. Interestingly, cotransfection with *Stim* also decreased the initial delay to the onset of current development (Fig. 3 *A*, *E*, and *F*). Together, these results show that overexpression of *olf186-F* is sufficient to increase CRAC current density, that coexpression with *Stim* produces a further enhancement, and that interaction with *Stim* may be the rate-limiting step for channel activation.

Apart from much larger current amplitudes, the Ca^{2+}-selective current in cells cotransfected with *olf186-F* and *Stim* exhibited biophysical properties that were indistinguishable from native CRAC currents. Monovalent ion selectivity upon removal of external Ca^{2+} (divalent-free), Na^+ current inactivation, and potentiation of Ca^{2+} current upon readdition of external Ca^{2+} were similar to that described for native CRAC current in lymphocytes and S2 cells (see Fig. 7*A*, which is published as supporting information on the PNAS web site) (4, 17–19). Current–voltage relations for the monovalent Na^+ current also showed inward rectification and a reversal potential of +45 mV (Fig. 7*B*), the same as native monovalent CRAC current and consistent with low permeability to Cs^+ (4). The response to voltage steps was also the same, with currents that increase slightly at very negative potentials (Fig. 7 *C* and *D*), as seen previously in S2 cells (4). Furthermore, the Ca^{2+} current in *olf186-F* + *Stim* transfectants was sensitive to pharmacological agents that act on native CRAC currents (Fig. 7 *E* and *F*). Gd^{3+} (50 nM) and 2-aminoethyldiphenyl borate (2-APB; 20 μM) blocked the enhanced Ca^{2+} currents, and at lower concentration (5 μM) 2-APB exhibited a characteristic potentiation of current before blocking. In summary, the ion selectivity, development and inactivation kinetics, and pharmacological profile of the large induced Ca^{2+} current after overexpression of *olf186-F* plus *Stim* match native CRAC currents. Because the current is not enhanced by overexpression of *Stim* alone, these findings support the possibility that *olf186-F* itself is part of the channel.

Effects of *Ca-P60A*, *Syx5*, and *tsr* dsRNA Treatment on Ca^{2+} Dynamics and CRAC Current. The SERCA pump also emerged from the RNAi screen as a putative regulator of SOC influx. However, because the screen was based on Ca^{2+} influx induced by TG (which blocks the SERCA pump), we were concerned about the potential for a false-positive hit. We therefore performed single-cell Ca^{2+} imaging and patch–clamp experiments using alternative stimuli (ionomycin, passive stores depletion) to deplete the Ca^{2+} store. Selective lowering of *Ca-P60A* mRNA was first verified by RT-PCR (Fig. 6*B*). Knockdown of *Ca-P60A* significantly increased resting $[Ca^{2+}]_i$, reduced the store release transient upon addition of TG and strongly suppressed Ca^{2+} influx upon readdition of external Ca^{2+} (Fig. 4 *A* and *B*). In addition, ionomycin in zero-Ca^{2+} solution applied to control cells evoked a sharp Ca^{2+} release transient with a peak that averaged ≈200 nM, but a greatly reduced release transient in *Ca-P60A* dsRNA-treated cells (Fig. 4 *C* and *D*), indicating reduced Ca^{2+} store content as a consequence of reduced SERCA pump activity. As shown by the summary of Ca^{2+} imaging experiments (Fig. 4*E*), knockdown of SERCA has a strong Ca^{2+} phenotype, raising resting $[Ca^{2+}]_i$, reducing release transients, and suppressing

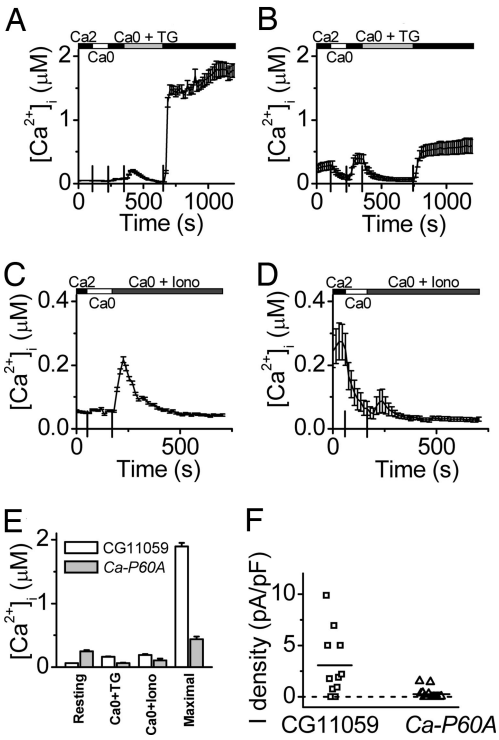

Fig. 4. Effects of *Ca-P60A* dsRNA on Ca^{2+} dynamics in individual S2 cells. (*A*) Averaged $[Ca^{2+}]_i$ in cells treated with control CG11059 dsRNA. (*B*) Averaged $[Ca^{2+}]_i$ in cells treated with *Ca-P60A* dsRNA. (*C* and *D*) Ca^{2+} release evoked by 1 μM ionomycin in control cells and in cells treated with *Ca-P60A* dsRNA to knock down SERCA expression. (*E*) Averaged $[Ca^{2+}]_i$ values ± SEM for control cells (white bars) and *Ca-P60A* dsRNA-treated cells (gray bars) labeled as in Fig. 2*D* and including peak $[Ca^{2+}]_i$ during ionomycin-evoked release transient (Ca0 + Iono). (*F*) Summary of inward CRAC current densities in control CG11059- and *Ca-P60A* dsRNA-treated cells ($P = 0.002$), using the same plotting format as in Fig. 2*F*.

influx evoked by TG. Furthermore, patch–clamp experiments demonstrated that CRAC currents also were suppressed when stores were depleted passively by dialysis of a Ca^{2+} chelator (Fig. 4*F*), confirming a requirement of *Ca-P60A* for activation of functional CRAC channels.

Several trafficking proteins also were identified as putative regulators of SOC activity (Table 2). *Syx5* is a syntaxin, several of which have been implicated in SNARE complexes that regulate vesicle trafficking; and *tsr* is referred to as an actin-binding protein that regulates cytoskeleton remodeling. A putative role of its human homolog, cofilin, has been reported in activation of store-operated calcium entry in platelets (20). Both *Syx5* and *tsr* dsRNA preincubation caused significant and selective lowering of mRNA levels (Fig. 6 *C* and *D*) and a corresponding inhibition of TG-dependent Ca^{2+} influx in S2 cells, without altering the resting $[Ca^{2+}]_i$ or store release (compare Fig. 5 *A*–*C*). Fig. 5*D* summarizes the inhibition of TG-evoked $[Ca^{2+}]_i$ influx when *Syx5* or *tsr* expression was knocked down. Patch–clamp experiments confirmed that CRAC currents were indeed suppressed during passive stores depletion when *Syx5* was knocked down, but effects of *tsr* knockdown on CRAC currents did not achieve statistical significance (Fig. 5*E*).

Discussion

Our genome-wide screen, based on direct Ca^{2+} influx measurements, validated *Stim* and identified several additional genes that are required for CRAC channel activity. We independently identified *olf186-F* (*Orai*) as essential for Ca^{2+} signaling and

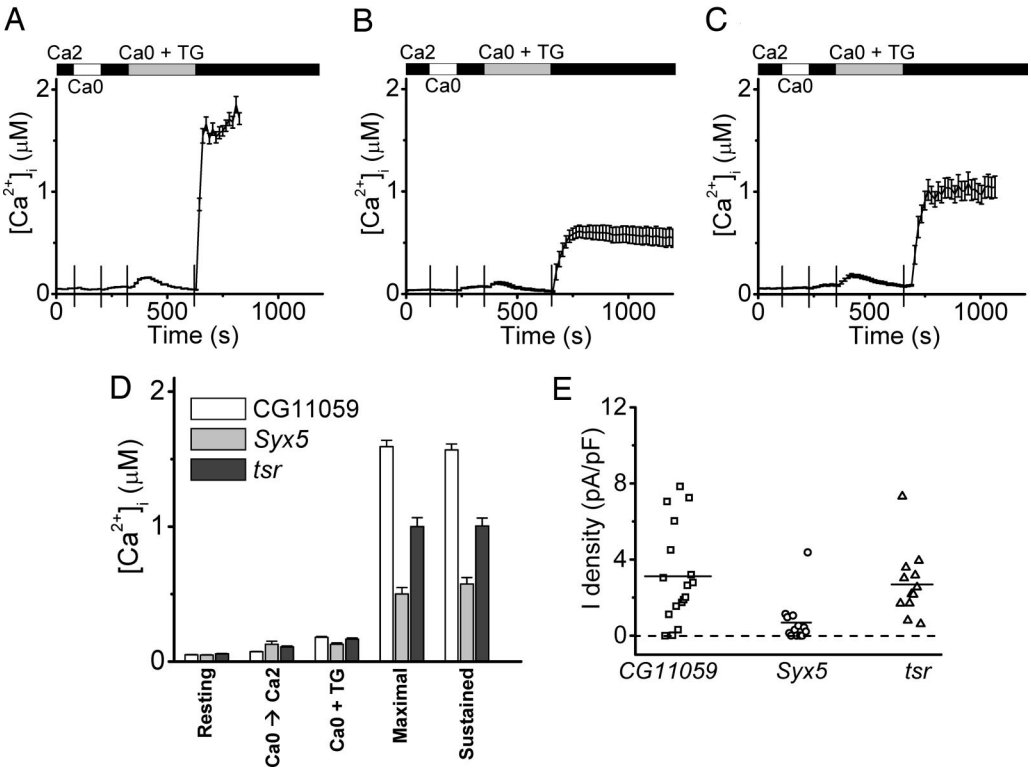

Fig. 5. Suppression of Ca^{2+} influx and CRAC current by *Syx5* and *tsr* dsRNA. (*A–C*) Averaged $[Ca^{2+}]_i$ in cells treated with control CG11059 dsRNA (*A*), *Syx5* dsRNA (*B*), or *tsr* dsRNA (*C*). (*D*) Averaged $[Ca^{2+}]_i$ values ± SEM for control cells (white bars), *Syx5* dsRNA-treated cells (gray bars), and *tsr* dsRNA-treated cells (black bars) labeled as in Fig. 2*D*. (*E*) Summary of inward CRAC current densities in *Syx5* and *tsr* dsRNA-treated cells, using the same plotting format as in Fig. 2*F*. Mean values for CG11059 and *Syx5* are significantly different ($P = 0.004$). The mean values for CG11059 and *tsr* are not significantly different ($P = 0.65$).

activation of CRAC current in S2 cells, confirming two recent reports (15, 21). In addition, we provide evidence based on overexpression that it may form an essential part of the CRAC channel. In mammalian cells overexpression of STIM1 increases Ca^{2+} influx rates and CRAC currents by ≈2-fold (7, 8), but in S2 cells we show that overexpression of *Stim* alone does not increase CRAC current, consistent with *Stim* serving as a channel activator rather than the channel itself. In contrast, transfection of *olf186-F* by itself increased CRAC current densities 3-fold, and cotransfection of *olf186-F* with *Stim* resulted in an 8-fold enhancement and the largest CRAC currents ever recorded. These results support the hypothesis that *olf186-F* constitutes part of the CRAC channel and that *Stim* serves as the messenger for its activation. Consistent with this hypothesis, the CRAC channel activation kinetics during passive Ca^{2+} store depletion were significantly faster with cotransfected *Stim*. Many fundamental aspects of the mechanism of CRAC channel activation remain to be clarified, including the protein–protein interactions that underlie trafficking and channel activation. Site-directed mutagenesis in a heterologous expression system may help to define the putative pore-forming region.

Similar to *Stim*, knockdown of *olf186-F* did not produce a severe cell growth phenotype (data not shown). It was neither a hit in a previous screen of cell survival (9) nor in any other published *Drosophila* whole-genome RNAi screen (10–14). The *olf186-F* gene is a member of a highly conserved gene family that contains three homologs in mammals, two in chicken, three in zebrafish, and one member only in fly and worm (see Fig. 8*A*, which is published as supporting information on the PNAS web site). C09F5.2, the only homolog in *Caenorhabditis elegans*, is expressed in intestine, hypodermis, and reproductive system as well as some neuron-like cells in the head and tail regions (www.wormbase.org). Worms under RNAi treatment against C09F5.2 are sterile (22). Analysis of hydrophobic regions of the predicted protein from the fly gene and the three mammalian homologs (Fig. 8*B*) suggested the presence of four conserved transmembrane segments. Cytoplasmic C termini are suggested by the presence of coiled-coil motifs in each sequence. A predicted transmembrane topology and the sequence for the fly gene are shown in Fig. 8*C*. Sequence alignment between members from human, chicken, and fly revealed strong sequence conservation in putative transmembrane regions and conserved negatively charged residues in loops between transmembrane segments. All three human members are expressed in the immune system (GNF Symatlas; http://symatlas.gnf.org/SymAtlas). Mutation of a human homolog of *Drosophila olf186-F*, *ORAI1* on chromosome 12, appears to be the cause of defective CRAC channel activity in severe combined immune deficiency patient T cells (15), consistent with a requirement for functional CRAC channels in the immune response. Interestingly, microarray data from public databases (GEO profiles; www.ncbi.nlm.nih.gov) combined with tissue-specific EST counts show that all three human members are expressed in a variety of nonexcitable tissues including thymus, lymph node, intestine, dermis, and many other tissues including the brain, although expression patterns and levels are different among the three members.

Ca-P60A has been proposed to be the only *Drosophila* SERCA gene (23). We validated its ER pump function by showing that ionomycin did not induce significant store release from S2 cells pretreated with dsRNA against *Ca-P60A*, consistent with a previous report (23). The elevation in resting $[Ca^{2+}]_i$ and rapidly changing Ca^{2+} transients during changes in external Ca^{2+} before addition of TG may indicate a low level of constitutive CRAC channel activity induced by store depletion. In addition, SERCA knockdown inhibited CRAC channel activity after passive store

depletion in whole-cell patch recordings. These results are consistent with the SERCA pump being required for normal activity of CRAC channels but do not rule out indirect inhibition of CRAC current as a consequence of residual high resting $[Ca^{2+}]_i$ or store depletion. The role of SERCA in CRAC channel function merits further study.

Among the hits, several are known to be involved in protein trafficking. The gene products of both *Syx5* and *Syx1A* are t-SNARE proteins involved in vesicle fusion in many cell types. We verified the RNAi effects of *Syx5* at the single-cell level and demonstrated strong suppression of CRAC channel activity as well as the SOC influx. *tsr* may regulate SOC influx indirectly by controlling cell metabolism because RNAi of *tsr* did not significantly influence CRAC current density in whole-cell patch–clamp experiments. Membrane trafficking previously was suggested to be important for SOC channel activity in *Xenopus* oocytes, based on inhibition by botulinum toxin or by a dominant-negative SNAP-25 construct (24), and our results further suggest a requirement for syntaxins and SNARE-complex formation, possibly to mediate translocation of *Stim* to the plasma membrane (6, 7). The screen also revealed three other groups of hits that may influence calcium dynamics. These results set the stage for experiments targeting specific genes to understand the fine tuning of Ca^{2+} homeostasis and signaling.

Methods

Drosophila S2 cells were cultured in 384-well plates containing $\approx$0.25 μg of dsRNA ($\approx 10^4$ cells per well). Each plate included a well with dsRNA targeting *Stim* as a positive control. After 5 days, cells were loaded with a $[Ca^{2+}]_i$ indicator fluo-4/AM (10 μM; Molecular Probes); free dye then was washed by Ringer solution containing 2 mM Ca^{2+} (see Table 3, which is published as supporting information on the PNAS web site, for all solution recipes). Three fluorescence measurements were systematically performed: basal (resting intracellular free Ca^{2+}), CCE (TG-dependent Ca^{2+} influx assessed 4 min after addition of TG), and F_{max} (maximal fluorescence 15 min after addition of Triton X-100 to a final concentration of $\approx$2% to detect changes in cell number). A schematic diagram is shown in Fig. 9*A*, which is published as supporting information on the PNAS web site. Values of "basal/F_{max}" were calculated for each well to indicate the normalized resting $[Ca^{2+}]_i$ level, and values of "CCE/basal" were computed to represent the relative CCE levels. The screen was carried out in duplicate. To correct for variation in dye loading or cell number, we computed ratios of fluorescence values (CCE/basal) as an index for Ca^{2+} influx evoked by TG. A scatter plot showed reasonable agreement for the replicate assays for most amplicons (Fig. 9*B*), particularly for hits with reduced Ca^{2+} influx reflected in lower CCE/basal values. Because most amplicons did not influence the dynamics of Ca^{2+} signaling, the average for a given plate was very close to that of nontreated wells. Therefore, *z*-scores of basal/F_{max} and CCE/basal equal to the value of the well minus the average of the plate divided by the standard deviation for the plate were calculated for each well. The averaged *z*-scores (Fig. 9*C*) represent variations in the distribution of CCE/basal measurements for each amplicon. Hits in the screen, defined by values of >3 standard deviations from the mean (*z*-score < -3 or >3) fell into four categories: (*i*) decreased resting $[Ca^{2+}]_i$; (*ii*) increased resting $[Ca^{2+}]_i$; (*iii*) decreased CCE (Table 2); and (*iv*) increased CCE. To eliminate false-positive outcomes, putative hits with a *z*-score of $F_{max} < -2$, or with more than five off-targets, were generally filtered out from the lists. Overlapping hits between groups *i* and *iv* and groups *ii* and *iii* were removed from group *iv* and *iii*, respectively.

The remaining methods can be found in *Supporting Materials and Methods* and Table 4, which are published as supporting information on the PNAS web site.

We thank Sindy Wei for help with $[Ca^{2+}]_i$ imaging; J. Ashot Kozak for helpful discussion; Karinne Cahalan for assistance with illustrations; Dr. Weihua Jiang for data processing; Dr. Luette Forrest for help with cell culture; and B. Mathey-Prevot, N. Perrimon, and staff at the *Drosophila* RNAi Screening Center at Harvard. This work was supported by National Institutes of Health Grant NS14609 (to M.D.C.), a George E. Hewitt Foundation fellowship (to S.L.Z.), and American Heart Association Scientist Development Grant 0630117N (to Y.Y.).

1. Prakriya, M. & Lewis, R. S. (2003) *Cell Calcium* **33,** 311–321.
2. Parekh, A. B. & Putney, J. W., Jr. (2005) *Physiol. Rev.* **85,** 757–810.
3. Gallo, E. M., Cante-Barrett, K. & Crabtree, G. R. (2006) *Nat. Immunol.* **7,** 25–32.
4. Yeromin, A. V., Roos, J., Stauderman, K. A. & Cahalan, M. D. (2004) *J. Gen. Physiol.* **123,** 167–182.
5. Roos, J., DiGregorio, P. J., Yeromin, A. V., Ohlsen, K., Lioudyno, M., Zhang, S., Safrina, O., Kozak, J. A., Wagner, S. L., Cahalan, M. D., *et al.* (2005) *J. Cell Biol.* **169,** 435–445.
6. Liou, J., Kim, M. L., Heo, W. D., Jones, J. T., Myers, J. W., Ferrell, J. E., Jr., & Meyer, T. (2005) *Curr. Biol.* **15,** 1235–1241.
7. Zhang, S. L., Yu, Y., Roos, J., Kozak, J. A., Deerinck, T. J., Ellisman, M. H., Stauderman, K. A. & Cahalan, M. D. (2005) *Nature* **437,** 902–905.
8. Spassova, M. A., Soboloff, J., He, L. P., Xu, W., Dziadek, M. A. & Gill, D. L. (2006) *Proc. Natl. Acad. Sci. USA* **103,** 4040–4045.
9. Boutros, M., Kiger, A. A., Armknecht, S., Kerr, K., Hild, M., Koch, B., Haas, S. A., Consortium, H. F., Paro, R. & Perrimon, N. (2004) *Science* **303,** 832–835.
10. DasGupta, R., Kaykas, A., Moon, R. T. & Perrimon, N. (2005) *Science* **308,** 826–833.
11. Agaisse, H., Burrack, L. S., Philips, J. A., Rubin, E. J., Perrimon, N. & Higgins, D. E. (2005) *Science* **309,** 1248–1251.
12. Baeg, G. H., Zhou, R. & Perrimon, N. (2005) *Genes Dev.* **19,** 1861–1870.
13. Bard, F., Casano, L., Mallabiabarrena, A., Wallace, E., Saito, K., Kitayama, H., Guizzunti, G., Hu, Y., Wendler, F., Dasgupta, R., *et al.* (2006) *Nature* **439,** 604–607.
14. Nybakken, K., Vokes, S. A., Lin, T. Y., McMahon, A. P. & Perrimon, N. (2005) *Nat. Genet.* **37,** 1323–1332.
15. Feske, S., Gwack, Y., Prakriya, M., Srikanth, S., Puppel, S.-V., Tanasa, B., Hogan, P. G., Lewis, R. S., Daly, M. & Rao, A. (2006) *Nature* **441,** 179–185.
16. Yagodin, S., Hardie, R. C., Lansdell, S. J., Millar, N. S., Mason, W. T. & Sattelle, D. B. (1998) *Cell Calcium* **23,** 219–228.
17. Lepple-Wienhues, A. & Cahalan, M. D. (1996) *Biophys. J.* **71,** 787–794.
18. Zweifach, A. & Lewis, R. S. (1996) *J. Gen. Physiol.* **107,** 597–610.
19. Christian, E. P., Spence, K. T., Togo, J. A., Dargis, P. G. & Patel, J. (1996) *J. Membr. Biol.* **150,** 63–71.
20. Redondo, P. C., Harper, M. T., Rosado, J. A. & Sage, S. O. (2006) *Blood* **107,** 973–979.
21. Vig, M., Peinelt, C., Beck, A., Koomoa, D. L., Rabah, D., Koblan-Huberson, M., Kraft, S., Turner, H., Fleig, A., Penner, R. & Kinet, J. P. (2006) *Science* **312,** 1220–1223.
22. Maeda, I., Kohara, Y., Yamamoto, M. & Sugimoto, A. (2001) *Curr. Biol.* **11,** 171–176.
23. Raymond-Delpech, V., Towers, P. R. & Sattelle, D. B. (2004) *Cell Calcium* **35,** 131–139.
24. Yao, Y., Ferrer-Montiel, A. V., Montal, M. & Tsien, R. Y. (1999) *Cell* **98,** 475–485.